Journal Homepage: http://ijcpe.uobaghdad.edu.iq
Iraqi Journal of Chemical and Petroleum Engineering
Vol. 25 No. 2 (June 2024) 17 – 31
EISSN: 2618-0707, PISSN: 1997-4884

Investigation of Wellbore Instability in Southern Rumaila Oil Field

Ali F. Zaidan [a, *], Farqad A. Hadi [a], Martin Klempa [b]

a Department of Petroleum Engineering, College of Engineering, University of Baghdad, Baghdad, Iraq
b Department of Geological Engineering, VSB - Technical University of Ostrava, Ostrava, Czechia

Abstract

This study aims to address the issue by providing valuable insights into the factors contributing to the wellbore instability and proposing effective measures to mitigate the problem in the southern part of the Rumaila oil field. A comprehensive one-dimensional mechanical earth model (1D MEM) was developed by utilizing various logs data from 4 wells across the south part of this field, including gamma ray, bit size, caliper, bulk density, and sonic compression and shear logs. The model was validated with laboratory tests, including Brazilin and Triaxial tests, as well as repeated formation tests. To analyze the wellbore stability, three different failure criteria, namely Mohr-Coulomb, Mogi-Coulomb, and Modified lade, were employed. The results indicated that the Mogi-Coulomb criterion was the most accurate failure criterion in predicting rock failure. Wellbore instability problems had been observed across the shale sections throughout the Rumaila oil field, particularly through Tanuma, Khasib, top and bottom of Ahmadi, Nahr Umr, and Upper Shale members and Middle Shale members of Zubair formations. The 1D MEM results indicated that Shaly formations exhibited low stiffness rocks (low Young's Modulus (YME)), low rock strength, and high Poisson's ratio (PR), suggesting potential challenges related to wellbore instability in the Tanuma, top and bottom of Ahmadi, Nahr-Umr, and Zubair formations. A sensitivity analysis was performed to determine the safest mud weight and the optimum well trajectory for future drilling operations. According to the updated mud window of this field in 2023, the pressure in the Mishrif and Zubair formations was reinforced by injection wells, as it was noted that the pressure behavior shifted from depletion (2000 Psi). Based on the findings of this study, the good inclination of (0-25°) can be drilled with the mud weight of 1.24-1.26 sg, while the good inclination of (25-40°) can be drilled with the mud weight of 1.28-1.30 sg in all directions (i.e., all azimuths). The stress regime in most of the formations was found to be a strike-slip to a normal fault regime. The findings of this study can significantly benefit the oil industry and enhance overall productivity.

Keywords: Rumaila oil field, wellbore instability, mud window, 1D-MEM, Mechanical earth model.

Received on 27/04/2023, Received in Revised Form on 25/08/2023, Accepted on 27/08/2023, Published on 30/06/2024

https://doi.org/10.31699/IJCPE.2024.2.2

1- Introduction

Rumaila oil field is one of the largest oil fields in Iraq, having been discovered in 1953. It is situated 50 kilometers west of Basra city, in southern Iraq, and spans an area of 1600 kilometers squared (Km^2). This area extends from the Iraq-Kuwait border in the south to the West Qurna oilfield in the north. The 8 1/2" hole section of this field is normally exposed to instability issues through drilling operations. This presents the risk of wellbore instability, which can result in surface subsidence, damage to subsea equipment or surface production facilities, and obstruction of production liners, creating challenges during the completion and production phases, [1-3]. The stress level in the subsurface has an impact on a variety of operations during the lifecycle of an oilfield. Such changes in near-wellbore tensions can lead to wellbore mechanical instability, [4]. Issues with instability include tight holes, stuck pipes, lost circulation, inadequately cleaned holes, and holes with poor cement, [5]. These problems can be attributed to the alteration of the stress level at the subsurface, especially at the wellbore. The increasing need to drill wells with complex trajectories, such as highly deviated, multilateral, and horizontal wells, is another reason for these drilling problems. Additionally, drilling in places with strong tectonic activity and depleted reserves increases the difficulty of maintaining the wellbore stability [6, 7]. Fig. 1 shows the lithologic column of the Rumaila oilfield and the associated downhole problems [8].

Geomechanics is a scientific discipline that explores the intricate interplay between the geological factors and the mechanical properties of rock, [9]. Reservoir geomechanics is a branch of geoscience in which rock deformation as a response to changes in stresses can be studied for further applications related to wellbore stability analysis, sand production, fault reactivation, and hydraulic fracturing. Studying how the rocks behave under different circumstances and determining the optimum weight to prevent that may significantly reduce

*Corresponding Author: Email: ali.zaidan2008m@coeng.uobaghdad.edu.iq

stability difficulties by building a mechanical earth model (MEM). This model predicts the level of stress as well as rock elastic characteristics and strength parameters. To build a 1D mechanical earth model, a rock mechanical analysis can assist in identifying the state of stresses surrounding the wellbore [10, 11]. The main result of 1D MEM is construction a safe mud weight and an optimum wellbore trajectory to minimize or control the rock failure. The main objective of this is to construct 1D geomechanical models (using Techlog 2021 software) for the development of drilling integrity in the Rumaila oil field, specifically focusing on optimizing mud weight selection. The analysis focused on an 8 ½" hole section for reservoir characterization and development, utilizing data from 4 wells across the field, and thus reduce NPT and drilling expenses in the Rumaila oil field.

Age		Group	Formation	Lithology	Description	Average thickness (m)	Mega sequence	Super sequence	Tectonic events
Period	Epoch								
Tertiary	L. Miocene-Recent	Kuwait	Dibdibba		Sand & pebble	200	AP 11	IV	Zagros orogeny
	Early-M Miocene		Lower fars		Clay St, Lst arg	170			
			Ghar		Sand & subround pebble occ Clay	110		III	
	M-L Eocene	Hasa	Dammam		Dolomite, porous vuggy	210	AP 10	I	Neo-Tethys Ocean closing
	Paleocene –Early Eocene		Rus		Anhydrite,white, massive interbedded w\ Dolomite	165			
			Umm-Er-Radhuma		Dolomite grey saccharoidol, inpart anhydritic	450			
Cretaceous	Late Cretaceous	Aruma	Tayarat		Bituminous Shale at top, Dolomite, grey	220	AP 9	VI	
			Shiranish		Limestone marly	120			
			Hartha		Lst,gloc,Dol,porous,locally vuggy,Lst,grey ,arg.	180			
			Sadi		Limestone white, chalcky, fine, compact	260		V	
			Tanuma		Shale: black-brown fissile	50			Tethys Obduction
			Khasib		Limestone: grey shaly	45			
	Middle Cretaceous	Wasia	Mishrif		Limestone: white detrital, porous, rudist	150	AP 8	IV	Neo-Tethys Ocean opening
			Rumaila		Limestone:, grey, marly	100			
			Ahmadi		Shale: Dark grey, fissile w/ Limestone: grey	140			
			Mauddud		Limestone grey	110		III	
			Nahr Umr		Shale black inter. w/ Sst	270			
	Early Cretaceous	Thamama	Shuaiba		Lst , Dolmaite fracture	85		II	
			Zubair		Shale,fissile, w/ sandstone fine-m. grained, Silt st, Clay st.	400			
			Ratawi		Limestone with streaks of Shale	200		I	
			Yamama		Limestone, light grey	120			
Jurassic	UpperJurassic		Sulaiy		Limestone, argillaceous and marly	300			

Fig. 1. Stratigraphic Column of the Study Area [12]

- Analysis of the 8 1/2 " Section Breakdown Time

The analysis of productive time versus nonproductive time (NPT) for the northern and southern parts of the Rumaila oil field shows that 56% of the total NPT is in the intermediate section, 41% in the production section, and 3% in the surface section. The majority of the NPT in the intermediate section is because of lost circulation issues in the Dammam and Hartha formations. In the production section (i.e., 8 1/2"), the wellbore instability-related downhole issues accounted for 80% of the total NPT (41%) including stuck pipe, wireline stuck, tight

hole, casing, and pipe hung. In contrast, 20% of the total NPT is associated with other issues. The production section is primarily composed of different lithologies including shale, carbonate, and sandstone formations.

2- Methodology

A strength parameter of a rock specimen defines a stress magnitude at which the specimen fails under a specified type of stress. The different modes of failure are described in failure envelopes and occur at different stress states. For each type of failure, the critical stresses are given. There are typically three failure modes studied here: hydrostatic compression, tensional failure, and shear failure.

In three dimensions the stress state is defined via the second rank stress tensor $\boldsymbol{\tau}$ with 9 coefficients (Eq. 1).

$$\sigma = \begin{pmatrix} \sigma_{xx} & \tau_{xy} & \tau_{xz} \\ \tau_{yx} & \sigma_{yy} & \tau_{yz} \\ \tau_{xz} & \tau_{zy} & \sigma_{zz} \end{pmatrix} \quad (1)$$

The stress tensor can be transformed by a change in the basis of the matrix, which results in the transformed matrix having non-zero elements only on its diagonal. The new basis gives us the direction in which no shear stresses τ act on a rock and normal stresses σ are the only non-zero elements. The direction and magnitude of these principal stresses can be obtained by calculating the eigenvectors and eigenvalues of the original stress tensor (Eq. 2):

$$\sigma = \begin{pmatrix} \sigma_{xx} & 0 & 0 \\ 0 & \sigma_{yy} & 0 \\ 0 & 0 & \sigma_{zz} \end{pmatrix} \quad (2)$$

Principal stresses can be denoted by decreasing index with decreasing magnitude as $\sigma_1 \geq \sigma_2 \geq \sigma_3$. In a field case, the principal stresses are obtained by a rotation of the stress vector. Further, it is typical that the highest principal stress is vertical, and the two other stresses are horizontal [13, 14].

As the strength of a rock can be expressed by one parameter only for a specific stress state as the strength of the rock (in the sense defined above) changes with the stress state. A frequently used representation of a stress state is Mohr's circle. It is constructed in the $\sigma - \tau$ space and represents a transformation for a plane stress problem. By choosing an orientation relative to a principal stress (horizontal axis) we can illustrate the magnitude of normal and shear stresses acting in a plane in that direction. The symbol τ describes the shear stress projected onto a 2D plane in the 3D stress vector, and the symbol σ represents the normal component on this plane. When the plane is rotated, we get the Mohr circles in Fig. 2.

Four wells in the south Rumaila oil field were chosen in this study. The wells were selected based on their location, input data quality and availability, calibration data such as drilling and mud log reports, and WBS events. The input data from the well logs, including gamma-ray, caliper and bit size, density, and sound logs, were first collected. The study involved an audit of the input data utilized to develop a geomechanical model for the 8½" section of the Rumaila oil field. Calculating the shale flag, vertical stress, hydrostatic pressure, pore pressure, rock mechanical properties, and in-situ stresses was the second stage in constructing the 1D MEM. The core test data, which include the Brazil and Triaxial tests to calibrate the results of rock mechanical properties, the RFT data to calibrate the results of pore pressure, and the mini-frac data to calibrate the results of horizontal stresses, were the data used to ensure the calibration of 1DMEM. Fig. 3 shows the workflow for constructing the 1D MEM which can be then highlighted in the following steps.

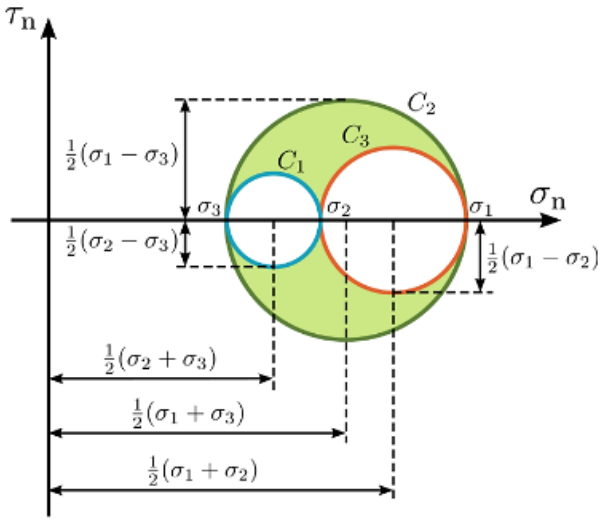

Fig. 2. Mohr's Circles for an Anisotropic Three-Dimensional Stress State [14]

2.1. Vertical stress

Overburden or vertical stress is the term used to describe the force exerted on a rock at any depth as a result of the weight of the rock and the fluid inside it. The determination of overburden stress at any depth based on density logs is simple (Eq. 3), where Sv is the vertical stress, ρ is the bulk density, and Z is the formation depth or formation thickness. Various methods can be employed to estimate the bulk density of formation; however, the extrapolated density approach (Eq. 4) can yield satisfactory outcomes for vertical stress [15], where ρ midline is the density at the seafloor or ground level, and Ao and α are the fitting parameters.

$$Sv = \int_0^z \rho\,(z)\ g\,dz \quad (3)$$

$$\rho\ extrapolated = \rho\ mudline\ + Ao \times (TVD - Air\ gap\ - Water\ Depth)^{\alpha} \quad (4)$$

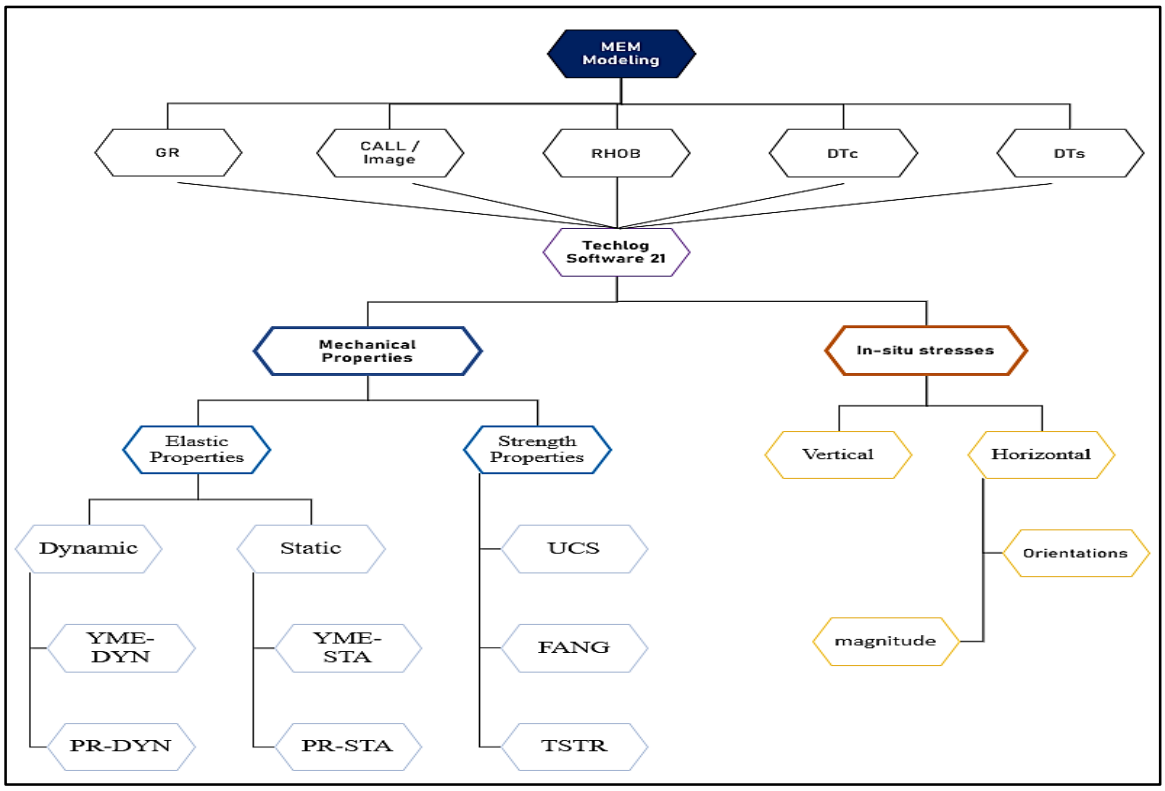

Fig. 3. Workflow of Mechanical Earth Model (1D-MEM)

2.2. Pore Pressure

Formation pressure is an essential parameter in various aspects of well planning and management, as it plays a critical role in determining the optimal drilling procedures [16]. There are two basic types of pore pressure: normal pressure or hydrostatic pressure, and anomalous pore pressure or geo-pressure, which exists in locations where there isn't a direct fluid flow to the neighboring regions. Two approaches are normally used to determine the geo-pressure: Eaton and bowers approach [17]. This study employed the Eaton approach, which was established by Eaton in 1975. The Eaton method, also known as Eaton's Geomechanical Stability Criterion, is a widely used approach to assess the stability of wellbores in geomechanics. It provides a criterion to evaluate the likelihood of wellbore failure based on rock strength and in-situ stresses. The method is particularly useful for analyzing the stability of deviated or horizontal wellbores. The Eaton method consists of two main equations (as defined in Eqs.5 and 6). This study utilizes acoustic logs (sonic logs) to determine the pore pressure gradient (Eq. 5) [18-20].

$$\frac{p}{D} = \frac{S}{D} - \left[\frac{S}{D} - \left({}^{P}/_{D}\right)_{n}\right]((\Delta\, tn)/(\Delta\, to))^{3} \quad (5)$$

$$\frac{p}{D} = \frac{S}{D} - \left[\frac{S}{D} - \left({}^{P}/_{D}\right)_{n}\right]((Ro)/(Rn))^{1.2} \quad (6)$$

Where Pp is pore pressure; D is depth; S is the stress (typically, Sv); and the subscripts n and o refer to the normal and measured values of resistivity (R) and sonic delta-t (ΔT) at each depth. The exponents shown in Eqs. 5 and 6 are typical values that are often changed for different regions so that the predictions better match pore pressures inferred from other data.

A drained porous rock under an external load will compact. The resulting deformation is a product of a change in pore volume and the change of the volume of the mineral frame of the rock. Measuring a series of pore volumes of the rock with increasing load magnitude allows to express relationship between pore volume and confining pressure Pc with the compressibility c_{pc} (Eq. 7) [14]:

$$c_{pc} = -\frac{1}{V_p}\frac{\partial V_p}{\partial P_c} \quad (7)$$

Where the equation (Eq. 8) of Zimmerman (1991) can be used [21]. The first subscript denotes the volume that is being deformed by a load, i.e. b for the pore volume and b for bulk volume. The second letter in the subscript denotes the type of load being imposed on the sample and causing the volumetric deformation, i.e. b for pore pressure changes and c confining pressure changes. The relationship between compressibility is:

$$c_{bc} = c_m + \emptyset c_{pc} \quad (8)$$

where cm is the compressibility of the rock matrix, or in other words the mineral frame of the rock. The compressibility of the rock matrix is calculated as a reciprocal value of rock matrix bulk modulus (Km). The rock matrix bulk modulus is calculated as a weighted average of bulk moduli of individual minerals (Ki) with

the weights (wi) being the percentages of the mineral content in the rock, calculated by Eq. 9 [14]:

$$\frac{1}{c_m} = K_m = \sum_{i=1}^{n} K_i w_i \quad (9)$$

2.3. Rock Mechanical Properties

Young's modulus and Poisson's ratio are two elastic properties of rocks, whereas the characteristics of rock strength are cohesion, unconfined compressive strength, frictional angle, and tensile strength. These characteristics play a crucial role in constructing 1D MEM and thus in determining the optimum mud weight to maintain the wellbore stable. The mechanical rock features could be found directly from the laboratory procedure data, which was then utilized to calibrate the findings of this study [18, 22].

The dynamic characteristics must be firstly computed using the density log, shear log, and compression velocity logs because these static values cannot be obtained directly from log data. The dynamic shear modulus (G) and dynamic bulk modulus (K) were calculated using Eqs. 10 and 11, respectively. Dynamic Young's modulus and Poisson's ratio were estimated using Eqs. 12 and 13, respectively [23].

$$Gdyn = 13474.45 \frac{\rho_b}{(\Delta t\ shear)^2} \quad (10)$$

$$Kdyn = 13474.45 \frac{\rho b}{(\Delta tcomp)^2} - \frac{4}{3} Gdyn \quad (11)$$

$$Edyn = \frac{9\ Gdyn \times Kdyn}{Gdyn + 3\ Kdyn} \quad (12)$$

$$Vdyn = \frac{3\ Kdyn - 2\ Gdyn}{6\ Kdyn + 2\ Gdyn} \quad (13)$$

Where Gdyn is dynamic shear modulus Kdyn dynamic bulk modulus, Pb is bulk density in gm/cm^3 and t shear is sonic shear velocity while Edyn is dynamic young's modulus and Vdyn is dynamic Poisson ratio.

2.4. Horizontal Stress

At depth, the rock is subjected to axial or vertical stress, which causes it to tend to move horizontally. This movement has an effect on the two horizontal stresses (minimum and maximum). In the geomechanical model, it is vital to know which of these stresses are minimum or maximum. The minimum horizontal stress (Shmin) can only be determined via direct techniques, such as the min-frac test, leak-off test, or hydraulic test. There are various indirect methods that can be used to compute the minimum (Shmin) and maximum (SHmax) horizontal stresses.

The poro-elastic method is the most used model for determining horizontal stresses. This method uses static Young's modulus, Poisson ratio, Biot's constant, overburden stress, and pore pressure, as illustrated in Eqs. 14 and 15. It was created and utilized for the first time by Plumb in 1991 [18, 24].

$$\sigma_h = \frac{v}{1-v}\sigma_v - \frac{v}{1-v}\alpha P_p + \alpha P_p + \frac{E}{1-v^2}\varepsilon_h + \frac{vE}{1-v^2}\varepsilon_H \quad (14)$$

$$\sigma_H = \frac{v}{1-v}\sigma_v - \frac{v}{1-v}\alpha P_p + \alpha P_p + \frac{E}{1-v^2}\varepsilon_H + \frac{vE}{1-v^2}\varepsilon_h \quad (15)$$

Where σh and σH are the maximum and minimum horizontal stress, σv is the vertical stress in psi, Pp is pore pressure in psi, v is static Poisson ratio, E is the static Young's modulus, α is Biot's coefficient and εh and εH are the minimum and the maximum strain coefficients.

3- Results and Discussion

This section presents the results of 1D MEM for determining the optimum mud weights. The collapse volume was also determined. Mud weight along with well inclination and azimuth was also presented for future well planning.

3.1. Vertical Stress and Pore Pressure

Fig. 4 shows the results of vertical stress for four wells from ground level to Zubair formation in the Rumaila oil field. The current pore pressure/ fracture gradient (PPFG) window of the Rumaila oil field was used to calibrate the predicted pore pressure. Table 1 shows the results of the pore pressure for each formation.

Fig. 5 presents the predicted pore pressure for four wells within the Rumaila oil field using the Eaton method (1975), from the Sadi to the Zubair formations. Modular Formation Dynamic Tester or MDT data (blue points) that were taken in (2011-2016) were also added in Fig. 5 for a comparison with the current PPFG model. It is found that the pressure in the Mishrif and Zubair formations was reinforced by injection wells, as it is noted that the pressure behavior is shifted or deviated from depletion.

3.2. Rock Elastic Properties

The outcomes of the mechanical earth model for the Rumelia oil field are shown in Fig. 6. The results are synthesized well log that derived the elastic and strength rock properties for the 8½'' section of the Rumaila oil field. The results showed a huge variance in the rock's mechanical properties with the burial depth. The results have been further calibrated with rock mechanical core test results (YME-Core) and (PR-Core). The results revealed that there is a good match between the calculated and the actual Static Young's Modulus and Static Poisson's ratio through the wells for the same part of the Rumaila oil field. These properties are essential parameters for geomechanical applications including wellbore stability analysis, hydraulic fracturing, reservoir subsidence, and compaction as well as sand production.

3.3. Rock Strength Properties

Fig. 7 presents the results of Unconfined compressive strength (UCS), Tensile strength (TSTR), and Internal Friction angle (FANG) for four wells from the Sadi formation to the Zubair formation in the South of Rumaila oil field, calibrated with rock mechanical core tests, where we notice that there is a great agreement in the behavior of the determined rock strength properties through the wells for the same part of the field.

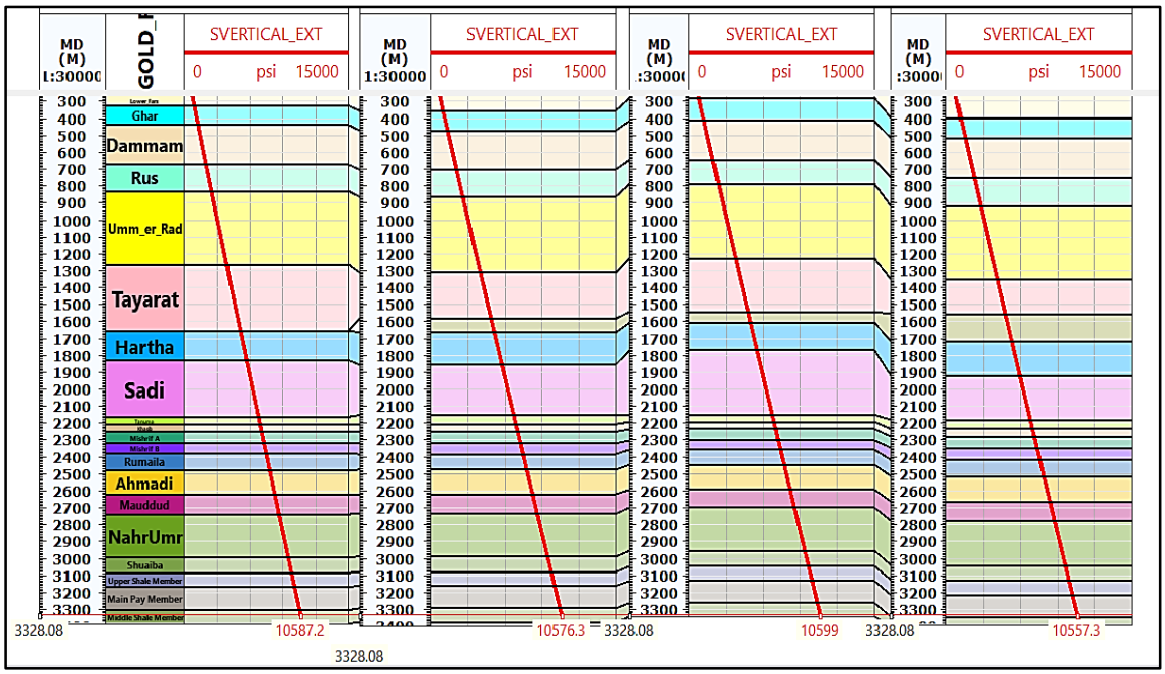

Fig. 4. Results of Overburden Stress (Ru-A, Ru-B, Ru-C, and Ru-D Respectively)

Table 1. The Predicted Pore Pressure Values for each Formation

NO.	Formation	Pore Pressure Range (Psi)
1	Sadi	2809- 3072
2	Tanuma	3365- 3510
3	Khasib	3410- 3582
4	Khasib Shale	3454- 3620
5	Mishrif	2540- 3753
6	Rumaila	3744- 3921
7	Ahmedi	3903- 4065
8	Mauddud	4102- 4283
9	Nahr Umr	4103- 4263
10	Shuaiba	4705 - 4854
11	Upper Shale	2392- 2964
12	Main Pay	3043 - 4289
13	Middle Shale	3832 - 4368

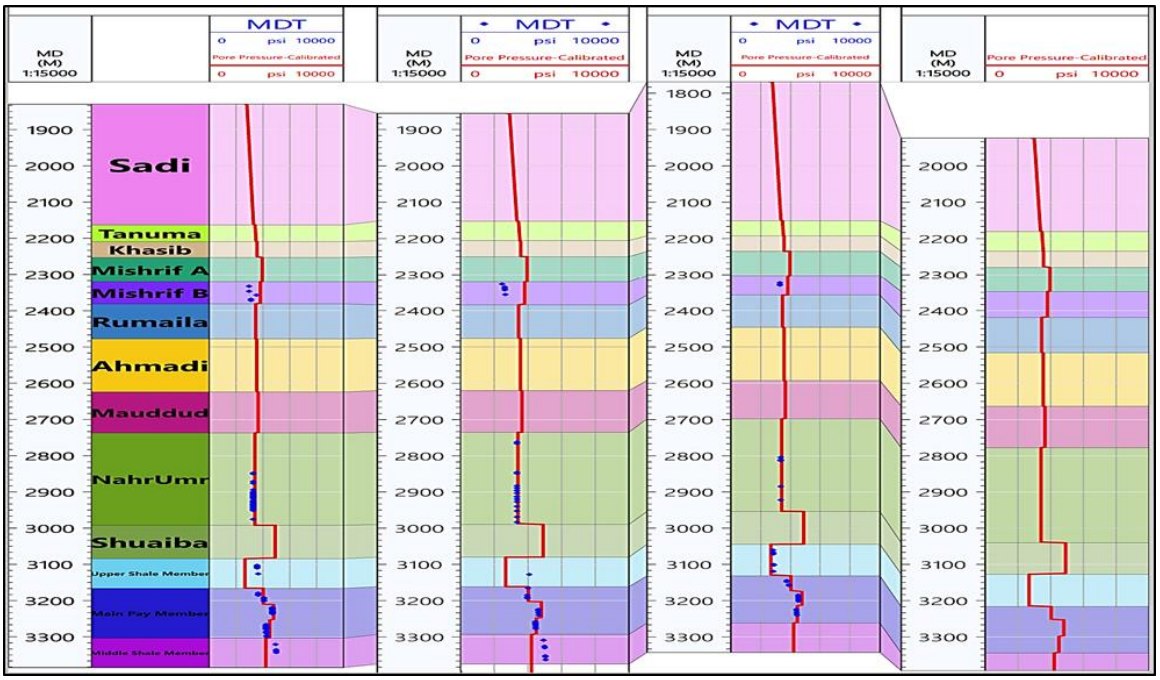

Fig. 5. Pore Pressure in Four Wells of South Rumaila (Ru-A, Ru-B, Ru-C, and Ru-D Respectively)

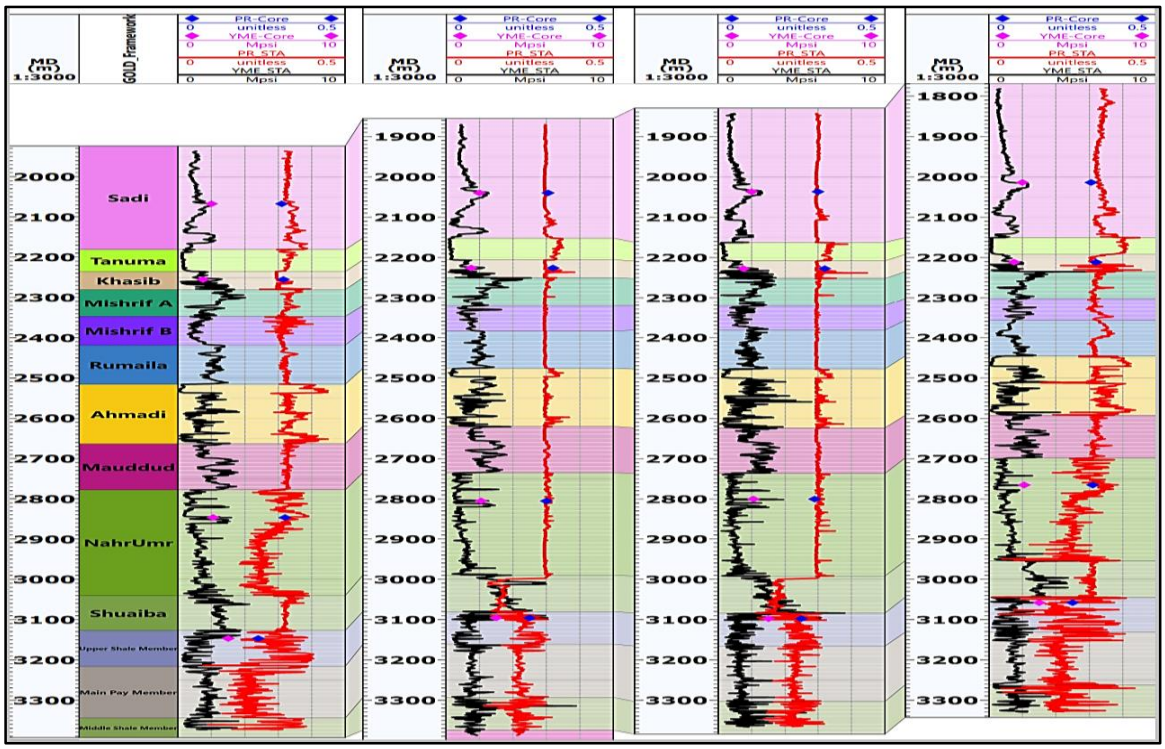

Fig. 6. Young's Modulus and Poisson's Ratio in Four Wells (Ru-A, Ru-B, Ru-C, and Ru-D Respectively)

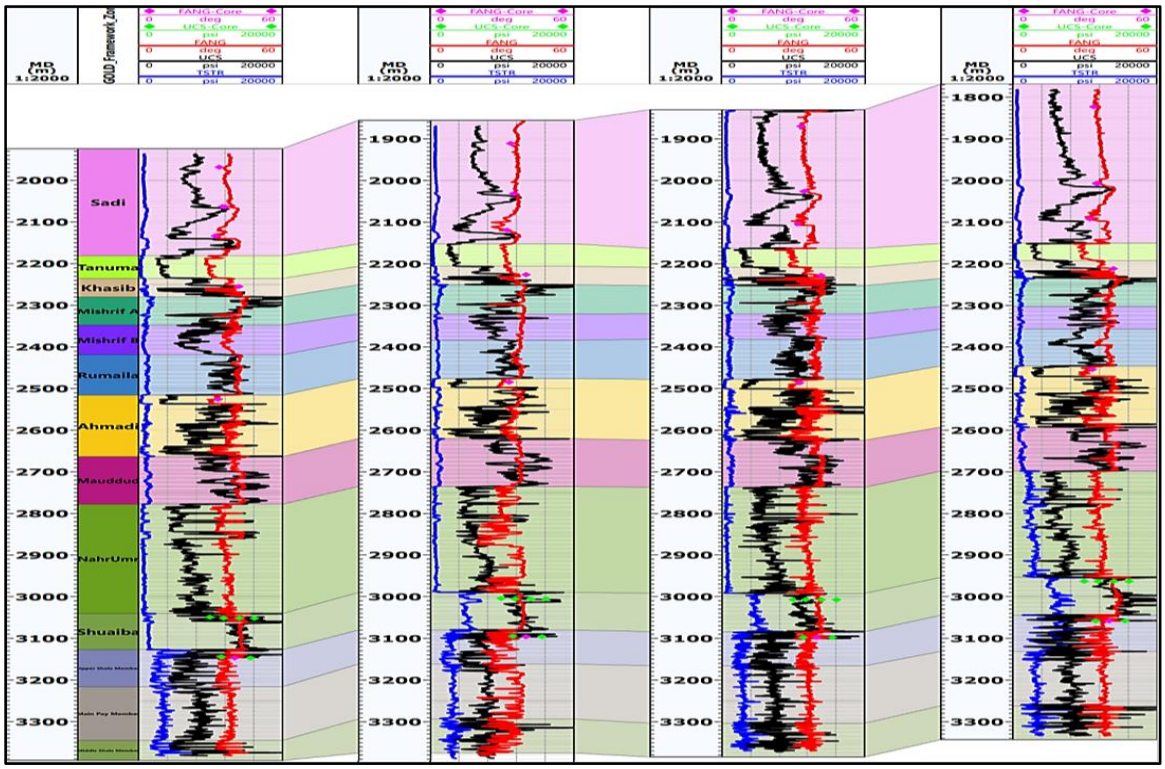

Fig. 7. Rock Strength Properties in Four Wells of South Rumaila (Ru-A, Ru-B, Ru-C, and Ru-D Respectively)

3.4. In-situ Principal Horizontal Stresses

The magnitudes of the horizontal stresses were calculated by using the Poro-elastic equations (Eqs. 14 and 15) as presented in Fig. 8. The magnitude of the minimum horizontal stress is then calibrated with the fracture pressure profile of PPFG model for each formation, which can help to constrain the lower limit for this model. In contrast, SHmax cannot be measured directly, it can be inverted using 3-shear Poro-elastic moduli, and even fracture using the Kirsch solution. Table 2 along with Fig. 8 summarizes the results of two horizontal stresses, vertical stress, as well as the fault regime results of section 8.5". The stress regime in the

majority of the formations was found to be the strike-slip to Normal fault regime, (*S*H > *S*V > *Sh*) and (*S*V > *S*H > *Sh*). The normal faulting regime was detected in the shaley and Sand formations that are represented in Tanuma and at the top and bottom of Ahmedi shale formations, Nhr Umr, and Zubair formations, while the strike-slip fault regime is observed against compacted formations such as Sadi, Khasib, and Mishrif carbonate formations.

Table 2. Faults Regime for Section 8.5" in Rumelia Oil Field

Formation	Avg. SHmax (Psi)	Avg. Shmin (Psi)	Avg. Sv (Psi)	Fault Regime
Sadi	6550	4750	6200	Strike Slip
Tanuma	5700	5240	7000	Normal
Khasib	7980	5370	7250	Strike Slip
Khasib-Shale	5700	5450	7350	Normal
Mishrif	9500	5650	7700	Strike Slip
Rumaila	10050	5810	7800	Strike Slip
Ahmedi-Top	6500	6010	7900	Normal
Ahmedi-Middle	8650	6200	8100	Strike Slip
Ahmedi-Bottom	7200	6350	8350	Normal
Mauddud	10200	6500	8750	Strike Slip
Nahr Umr	8400	6900	8950	Normal
Shuaiba	12000	7400	9700	Strike Slip
Top of USM	14100	6500	9800	Strike Slip
Middle & Bottom of USM	8000	6800	10250	Normal
Main Pay	9200	7000	10550	Normal
Middle Shale	12200	6950	10800	Strike Slip

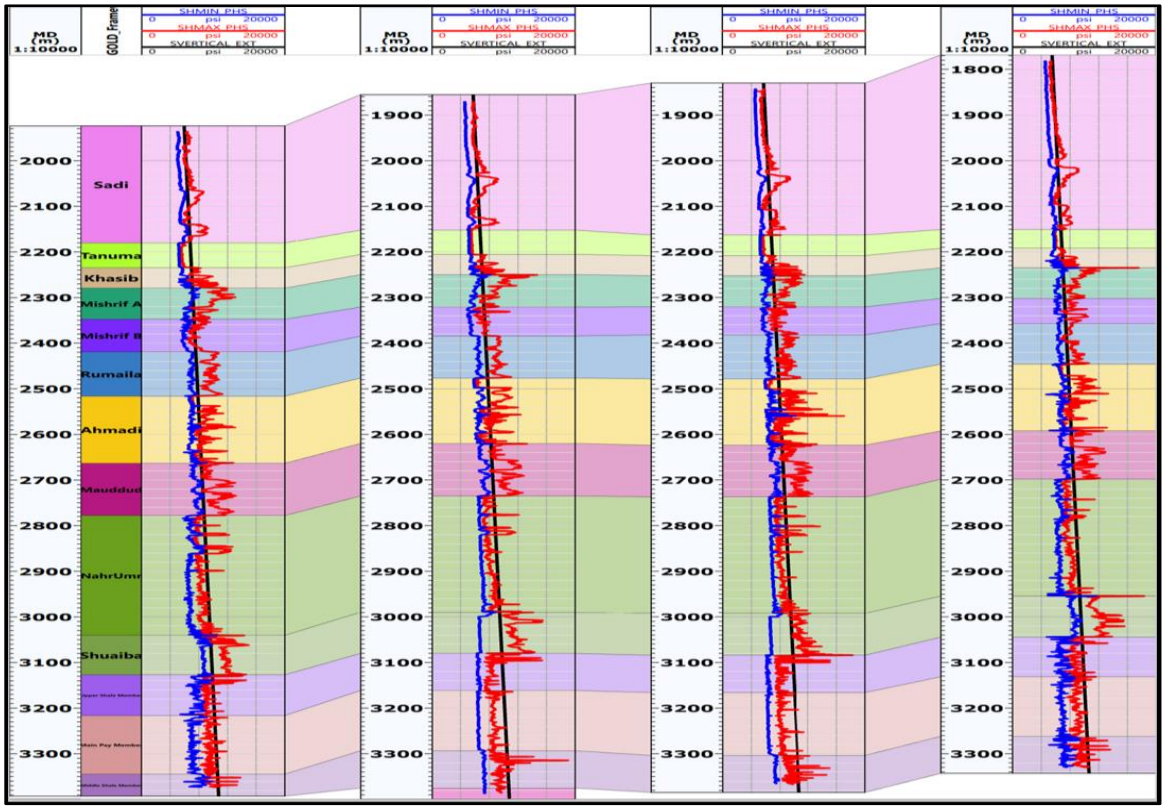

Fig. 8. Principal Stresses with MDT Data in Four Wells of South Rumaila (Ru-A, Ru-B, Ru-C, and Ru-D Respectively)

3.5. Wellbore Instability Analysis

It is important to utilize the failure criteria to determine the stress concentration around the wellbore to determine the threshold of the required mud weights to maintain the wellbore from either breakout or breakdown. In other words, by identifying the induced stress values, a safe drilling mud weight window, and a potential borehole failure can be determined based on the used mud weight and the applied failure criteria. Mohr coulomb, Mogi coulomb, and Modified Lade failure criteria were utilized to predict the rock failure along the production section. The Mohr-coulomb criteria showed an overestimation failure compared to the actual rock failure. On the other hand, the predicted failure by Modified Lade was less than the actual failure. The results of this study revealed that the Mogi-Coulomb failure criterion is highly compatible with the wellbore failure observations. As a result, this criterion has been selected to be used in the study. Four wells located in the southern part of the

Rumaila oil field have been chosen to be analyzed, along with their corresponding drilling events. The findings from this study will provide valuable insights for future well drilling operations.

Fig. 9 presents the rock failure of one well in Rumaila oil field in the following tracks based on Mogi approach that was also accompanying with the formation lithologies.

• *Track 1* shows the formations of the interested production section (8 ½").

• *Track 2* represents the mud weight window with the minimum horizontal stress indicated by the light blue color on the right side and the breakdown pressure gradient, lost circulation, and breakdown failure indicated by the dark blue color. Exceeding either or both of these limits can lead to potential drilling issues including tensile rock fracturing or lost circulation problems. On the left side, the grey color detects the mud weight limit that represents the kick, and the yellow color detects the mud weight limits that reveal the shear failure (breakout). Kick or shear failure may occur when the actual mud weight is lower than either or both of the limits mentioned earlier. To ensure a stable wellbore, the safe operating mud weight should be designed to be within the middle area (clean zone) of the mud weight window.

• *Track 3* shows the borehole caliper log as the actual failure calibration, the red zone indicates an oversize hole (washout or breakout), and the yellow zone indicates the under-gauge hole. The line separating the zones is the bit size which is 8 ½" in this study.

• *Track 4* displays the formation lithologies.

Actual failure calibration is employed to assess the validity of the applied failure criterion with the geomechanical model. These tracks indicated a good agreement between the predicted borehole failures with the wellbore calipers and actual drilling events which are recovered from daily drilling reports and final good reports. The drilling events are marked in tracks#2 and 3 at corresponding depths. For this well and other three wells, the wellbore instability problems had been observed across shale sections throughout the Rumaila oil field, particularly through Tanuma, top and bottom of Ahmadi, Nahr Umr, and Upper and Middle Shale members of the Zubair formation.

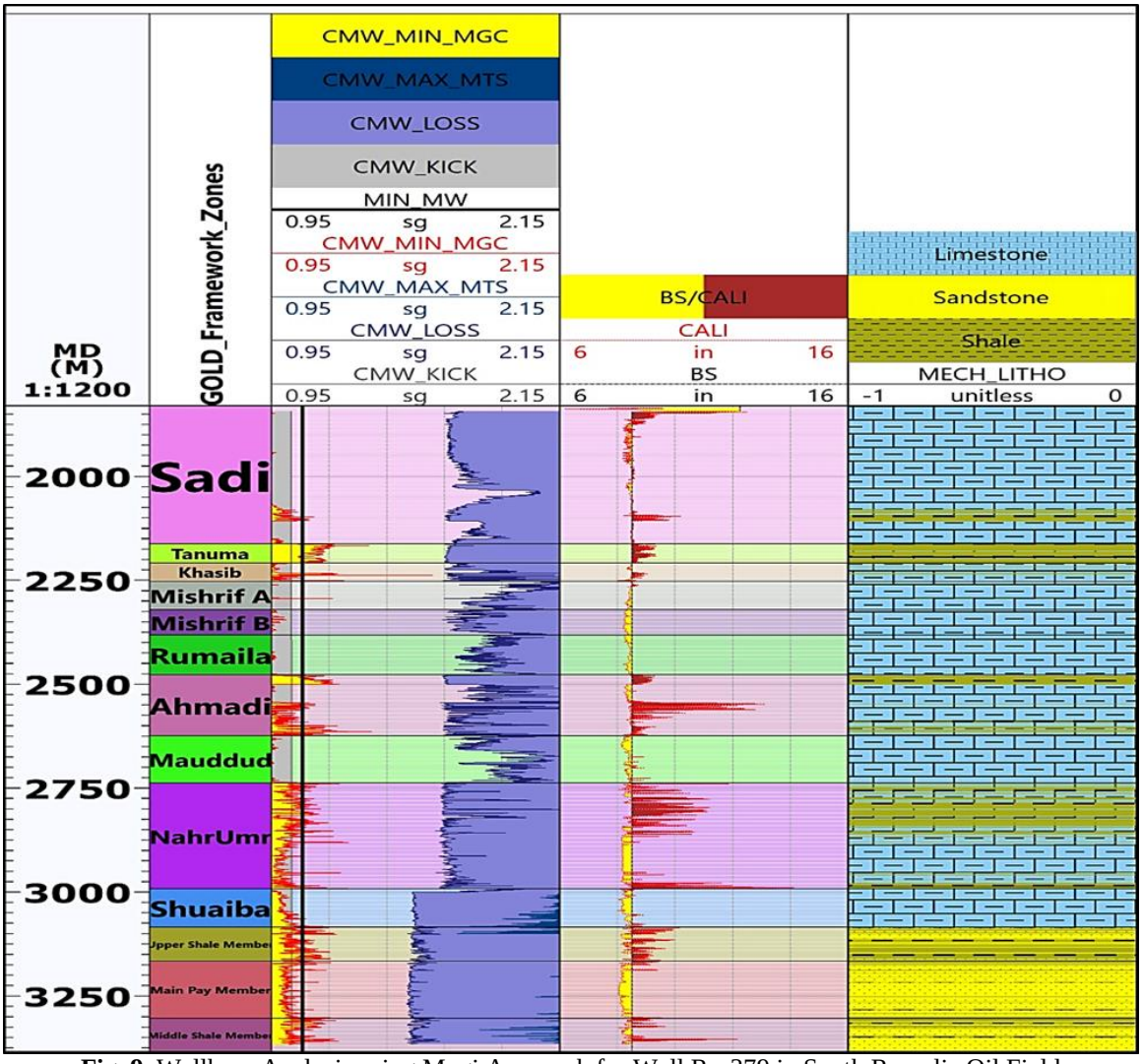

Fig. 9. Wellbore Analysis using Mogi Approach for Well Ru-379 in South Rumelia Oil Field

3.6. Borehole Collapse Volume Analysis

The caliper logs of 20 wells (10 wells of the Northern and 10 wells of the Southern of the Rumaila oil field) have been used to calculate the collapse volume from the top of the Sadi formation to the bottom of the Zubair formation. Fig. 10 shows the total collapse volume of these 20 wells; however, the thickness for each formation may be different, resulting a difficulty in comparing the collapse volumes of formations. To overcome this challenge, the collapse severity considering the formation thickness will be quantified by calculating the average collapse volume per 30m interval of each formation as presented in Fig. 11. The results of Fig. 10 showed that the volume of collapse in the shale sections (Tanuma, Khasib Shale, Ahmadi, Nahr Umr, and Zubair units) is similar between the wells drilled in the northern and southern parts of the field in each formation. Additionally, the limestone and sandstone formations in Rumaila are deemed to be sufficiently competent and are unlikely to contribute to premature wellbore collapse (Fig. 10 and Fig. 11), indicating that the rock characteristics and stresses are homogeneous, which confirms the possibility of using one mud weight window for the whole field. In contrast, limestone and sandstone formations in the Rumaila oil field, such as Sadi, Khasib, and Mishrif formations, are competent enough and it would not contribute to the premature wellbore collapse. The results of Fig. 11 also indicated that the Tanuma shaly formation has a relatively high average volume of collapse when compared to other shaly formations including Ahmadi and the upper shale of Zubair formation.

3.7. Sensitivity Analysis

A single-depth sensitivity analysis was conducted on the Tanuma Shale formation at critical depths where failure had occurred (at 2160 m depth) when the actual mud weight was used. This analysis revealed that shear failure occurred at the actual mud weight where the Tanuma formation has the lowest value of unconfined compressive strength of 2538 psi. Fig. 12 illustrates that a caliper size was 9.7" against the Tanuma failure interval.

The stereonet and line plots for Tanuma formation are visualized in Fig. 13 and Fig. 14, respectively. Fig. 13 a displays the minimum mud weight required to prevent the rocks from breaking out as a function of well azimuth and orientation. The plot indicates that the low deviation wells with an inclination of (0-40°) are stable in all directions. When the well inclination is increased to be (45-90°), the shear failure is expected to be occurred in both the minimum and maximum horizontal stresses directions. The maximum mud weight that required to prevent the formation from breakdown as a function of azimuth and deviation is also illustrated in Fig. 13 b. In terms of the tensile rock failure, a stereonet plot analysis revealed that wells inclined between 0-40° demonstrate greater stability, but the formation breakdown occurs more frequently in wells with inclinations greater than 60°.

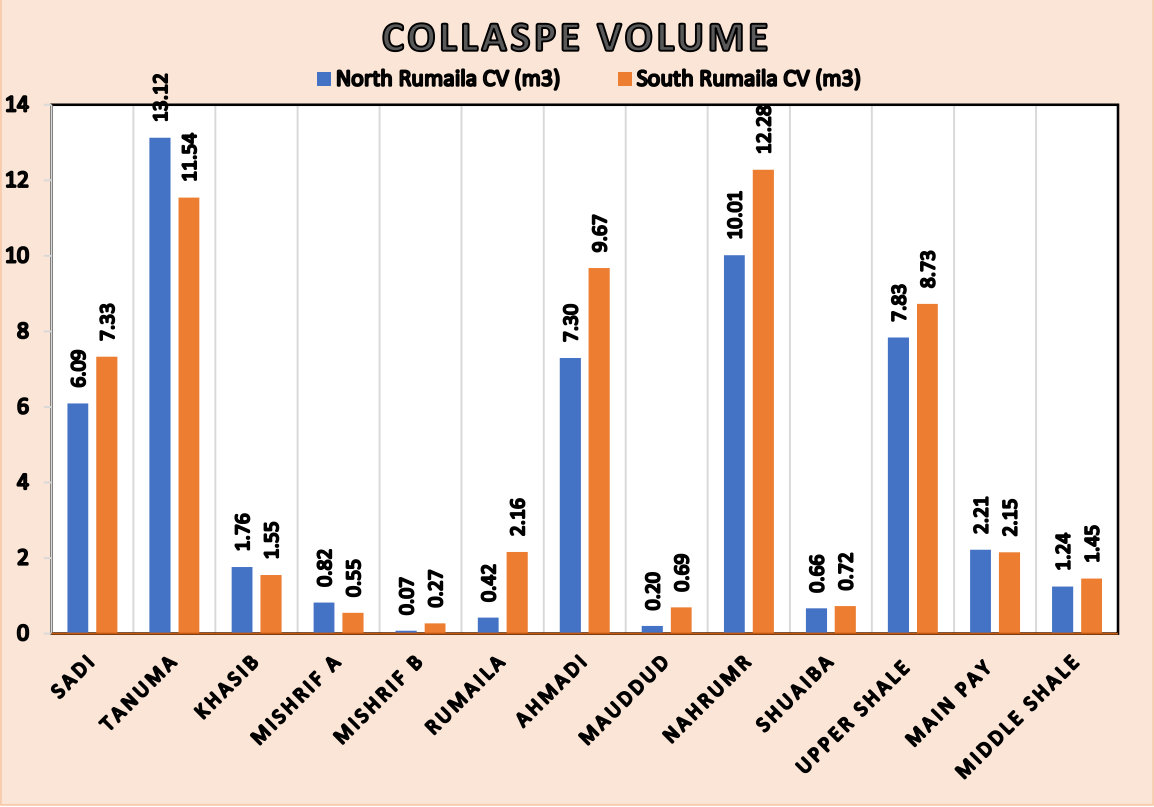

Fig. 10. Total Collapse Volume of 20 Wells

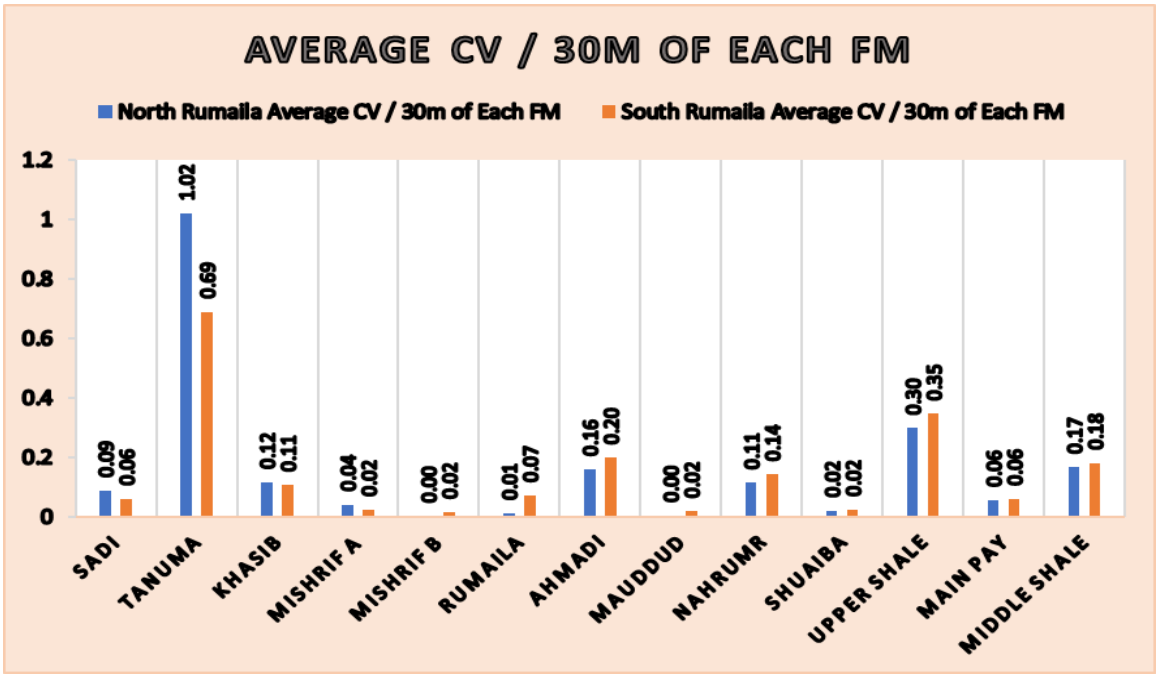

Fig. 11. Average Collapse Volumes per 30 m of each Formation for 20 Wells

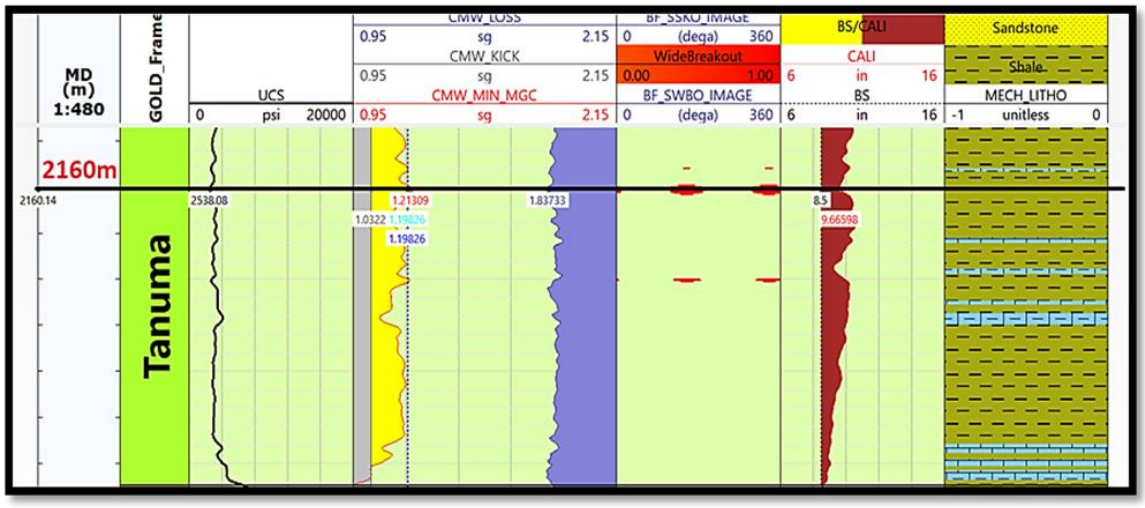

Fig. 12. Single Depth Sensitivity Analysis Designated Depth of 2160 m in Tanuma Formation

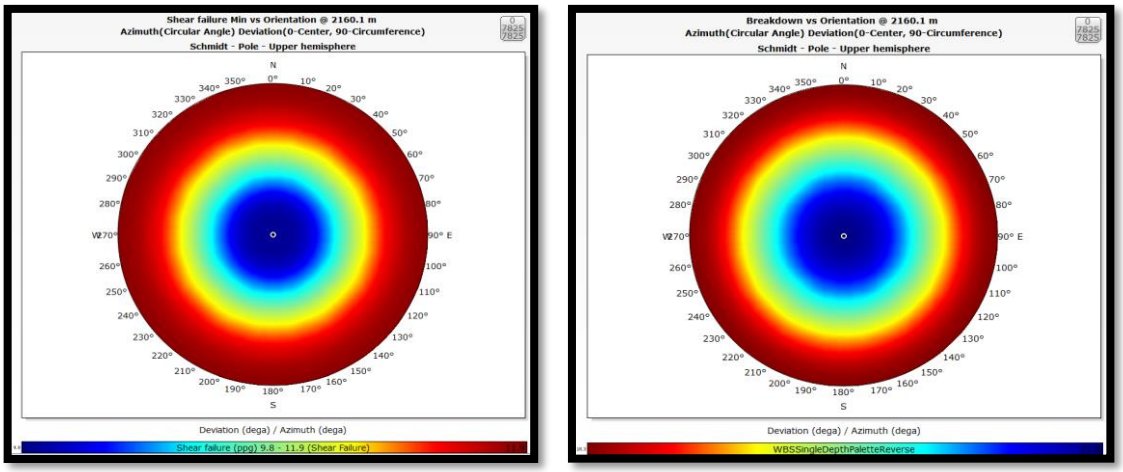

(a) (b)

Fig. 13. Breakout (a) and Breakdown (b) for Tanuma Formation at 2160 m

In Fig. 14, a line plot displays the mud weight window as a function of deviation ranging from 0-90°. The boundary line that separates the white and yellow regions represents the minimum mud weight required to prevent the rock breakout. Meanwhile, the boundary line between the blue and white regions represents the maximum mud weight that can be applied before the tensile rock fracturing. It is evident from the plot that the mud weight window narrows for inclinations greater than 25°. For wells with inclinations between 0-25°, mud weights range from 1.24-1.26 sg, while they are 1.28-1.30 sg for inclinations between 25-40°.

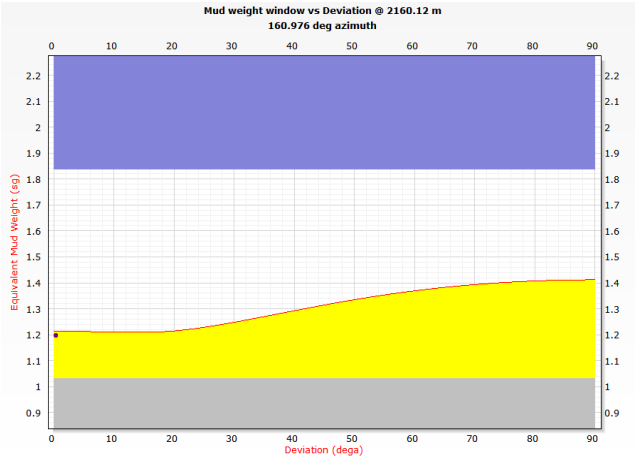

Fig. 14. Line Plot Sensitivity Analysis at a Depth of 2160 m for Tanuma Formation

3.8. Mud Weight Recommendations

Mud weight recommendations for drilling the formations from Sadi to Zubair (Vertical, S-shaped, and J-shaped wells) are outlined in Table 3 through Table 5. The conventional Zubair reservoir wells can be reached by using three casing strings at maximum inclination at 40° through from Sadi to Zubair formations. For drilling the horizontal wells, in contrast, higher mud weights are required to maintain the wellbore stable; therefore, four casing strings will be applied.

Table 3 summarizes the mud weights for vertical to moderately inclined wells with inclination angles up to 25° and in any azimuth. Furthermore, Table 4 summarizes the mud weights for wells with higher inclinations up to 40° through the Zubair formation and in any azimuth. For higher inclinations, the required MW is strongly dependent on the well azimuth. Table 5 provides mud weights recommended for a range of azimuths with an inclination higher than 40°. The results indicated that a significantly higher mud weight is required when drilling in the direction of Shmin. Therefore, the optimum orientation for reaching the Zubair reservoir is in the direction of SHmax with an azimuth range of 355° - 85° in North to Northeast direction and 175° - 265° in South to Southwest direction.

Table 3. Recommended Mud Weight for Well Inclination between (0-25 deg)

Required MW range (sg)	Formations
1.24 – 1.26	Tanuma, Khasib, Mishrif & Rumaila
1.24 – 1.27	Ahmadi, Mauddud, Nahr Umr & Shuaiba
1.26 – 1.30	Zubair

Table 4. Recommended Mud Weight for Well Inclination between (24-45 deg)

Required MW range (sg)	Formations
1.28 - 1.30	Tanuma, Khasib, Mishrif & Rumaila
1.28 – 1.32	Ahmadi, Mauddud, Nahr Umr & Shuaiba
1.30 – 1.33	Zubair

Table 5. Recommended Mud Weight Range for Wells Drilled at Angles Greater than 40° in Zubair Formation

Well Azimuth Range	Required MW (sg)	Recommendations
N355°- N30°	1.33 – 1.35	Highest MW is required for most northerly directed azimuths and decreases eastwards.
N30° - N60°	1.32 – 1.33	MW range consistent across azimuth range, consider use of higher value towards edges.
N60° - N85°	1.33 – 1.35	Lowest MW is required for smallest azimuths in range and increases eastwards.
N85° - N175°	1.35 – 1.38	Highest MW is required for most southerly directed azimuths and decreases westwards.
N175° - N210°	1.33 – 1.35	MW range consistent across azimuth range, consider use of higher value for higher inclination.
N210° - N240°	1.32 – 1.33	Lowest MW is required for smallest azimuths in range and increases northwards
N240° - N265°	1.33 – 1.35	Lowest MW is required for smallest azimuths in range and increases northwards
N265° - N355°	1.35 – 1.38	Highest MW is required for azimuths between N120°-N150° and decreases towards edges of range

4- Conclusions

The key findings from this study can be summarized in the following points:

- Based on the results of mechanical rock property analysis, formations including Tanuma, Ahmadi, Nahr-Umr, and Zubair exhibited a decrease in both Young's modulus and rock strength, along with an increase in Poisson's ratio, indicating a higher susceptibility to potential issues with wellbore stability.
- Based on the Modular Formation Dynamic Tester (MDT) data, it was found that the pressure in Mishrif and Zubair formations was reinforced by injection wells, and it was noted that the pressure behavior shifted or deviated from the depletion of 2000 Psi.

- The stress regime in the majority of the formations was found to be the strike-slip to Normal fault regime, (SH > SV > Sh) and (SV > SH > Sh).
- The wellbore instability problems had been observed across shale sections throughout the Rumaila Oil field, particularly through Tanuma, top and bottom of Ahmadi, Nahr Umr, and Upper and Middle Shale members of Zubair formation.
- The results showed that the collapse volume in shale sections (Tanuma, Khasib Shale, Ahmadi, Nahr Umr, and Zubair units) are almost convergent between the wells drilled in the northern and southern parts of the field in each formation, indicating that the rock characteristics and stresses are homogeneous.
- The limestone and sandstone formations in the Rumaila oil field are considered competent enough and are not likely to contribute to premature collapse of the wellbore.
- The wells with a low deviation of (0-40°) are consistently stable in all directions. Shear failure is anticipated when the inclination ranges from (45-90°) in both directions of the minimum and maximum horizontal stresses.
- With respect to the rock breakdown failure, the wells with inclinations of (0-40°) are more resistant to tensile failure, and the likelihood of a breakdown is expectedly higher when the inclination is more than 60°.
- The well with inclinations of (0-25°) can be drilled with the mud weight of 1.24-1.26 sg, while the wells with inclinations of (25-40°) can be drilled with the mud weight of 1.28-1.30 sg. in all directions for Tanuma formation.
- The preferred orientation of drilling is the direction of SHmax with an azimuth range of 355° - 85° in North to Northeast direction and 175° - 265° in South to Southwest direction.
- In deviated sections of the wellbore, there is an increase in the risk of chemical instability-related problems due to the potential for longer intervals and longer periods of exposure through reactive shale formations.

References

[1] M. A. Issa, F. A. Hadi, and R. Nygaard, "Coupled reservoir geomechanics with sand production to minimize the sanding risks in unconsolidated reservoirs," *Petroleum Science and Technology*, vol. 40, no. 9, pp. 1065-1083, 2022. https://doi.org/10.1080/10916466.2021.2014522

[2] M. A. Issa, and F. A. Hadi, "Estimation of Mechanical Rock Properties from Laboratory and Wireline Measurements for Sandstone Reservoirs," *The Iraqi Geological Journal*, vol. 54, no. 2D, pp. 125-137, 2021. https://doi.org/10.46717/igj.54.2D.10Ms-2021-10-29

[3] Z. Bashara, and F. Hadi, "Estimation of Shear Wave Velocity for Shallow Depth Using Artificial Neural Network Technique: A Case Study in Rumaila oil field," *Iraqi Geological Journal*, vol. 56, no. 1D, pp. 114-128, 2023. https://doi.org/10.46717/igj.56.1D.10ms-2023-4-19

[4] J. J. Zhang, "Applied petroleum geomechanics," *Applied Petroleum Geomechanics*. pp. 1–534, 2020, https://doi.org/10.1016/C2017-0-01969-9

[5] A. H. Dakhiel, and H. Abdul Hadi, "Integrated 3D Mechanical Earth Modelling to Intensively Investigate the Wellbore Instability of Zubair Oil Field, Southern Iraq," *The Iraqi Geological Journal*, vo. 54, no. 2E, pp.38-58, 2021. https://doi.org/10.46717/igj.54.2E.4Ms-2021-11-20

[6] J. Madhur, M. D. Zoback, and P. Hennings, "A scaling law to characterize fault-damage zones at reservoir depths," *AAPG Bulletin*, vol. 98, no. 10, pp. 2057-2079, 2014. https://doi.org/10.1306/05061413173

[7] C. G. Nmegbu and L. V. Ohazuruike, "Wellbore instability in oil well drilling: A review," *International Journal of Engineering Research and Development*, vol. 10, no. 5, pp. 11-20, 2014.

[8] W. J. Al-Mudhafar, and S.M Hosseini Nasab, "Lessons learned from IOR steam flooding in a bitumen-light oil heterogeneous reservoir," In *IOR 2015-18th European Symposium on Improved Oil Recovery, European Association of Geoscientists & Engineers*. 2015. https://doi.org/10.3997/2214-4609.201412113

[9] A. K. Faraj, and H. A. Abdul Hussein, "Application of Finite Element Technique: A Review Study," *Iraqi Journal of Chemical and Petroleum Engineering*, vol. 24, no. 1, pp.113-124, 2023. https://doi.org/10.31699/IJCPE.2023.1.13

[10] R. Plumb, S. Edwards, G. Pidcock, D. Lee, and B. Stacey, "The mechanical earth model concept and its application to high-risk well construction projects," In *IADC/SPE Drilling Conference*, 2000. https://doi.org/10.2118/59128-MS

[11] W. Al-Wardy, and O. P. Urdaneta,"Geomechanical modeling for wellbore stability during drilling Nahr Umr shales in a field in petroleum development Oman." In *Abu Dhabi International Petroleum Exhibition and Conference*. 2010. https://doi.org/10.2118/138214-MS

[12] P. Sharland, R. Archer, D. Casey, R. Davies, S. Hall, A. Heward, A. Horbuy, and M. Simmons,"Arabian plate sequences stratigraphy, an integrated approach," *GEO Arabia Special Publication*, vol.2, 2001.

[13] P. Bujok, M. Klempa, V. Slivka, M. Porzer, I. Nemec, V. Stastna, E. Smejkalova, J. Zdvorak, "Remediation of the Old Ecological Load in the Protected Area of the Morava River - Re-abandonment of the Oil and Gas Production Wells", *The Mining-Geology-Petroleum Engineering Bulletin*, Vol. 30, no. 1, pp. 1-8, 2015, https://doi.org/10.17794/rgn.2015.1.4

[14] M. Porzer, J. Sancer, M. Klempa, and A. Nermoen, "R4.2 Report on geomechanical data to be stored in the project database," CO2-SPICER - CO2 Storage Pilot In a CarbonatE Reservoir final report, 2022. http://dx.doi.org/10.2139/ssrn.4698108

[15] A. K. Faraj, and H. A. Abdul Hussein, "Vertical Stress Prediction for Zubair Oil Field/Case Study," *Journal of Engineering*, vol. 29, no. 2, pp.137-152, 2023. https://doi.org/10.31026/j.eng.2023.02.09

[16] A. K. AlHusseini, and S. M. Hamed-Allah, "Estimation Pore and Fracture Pressure Based on Log Data; Case Study: Mishrif Formation/Buzurgan Oilfield at Iraq," *Iraqi Journal of Chemical and Petroleum Engineering*, vol. 24, no. 1, pp.65-78, 2023. https://doi.org/10.31699/IJCPE.2023.1.8

[17] A. K. Faraj, and H. A. Abdul Hussein,"Calculation Pore Pressure Utilized Two Methods / Case Study of Zubair Oil Field," *Texas Journal of Engineering and Technology*, vol.11, pp.1-6, 2022.

[18] A. Abbas, F. Ralph, and M. Alsaba, "Geomechanical Modeling and Wellbore Stability Analysis Approach to Plan Deep Horizontal Wells Across Problematic Shale Formation," In *the SPE/AAPG/SEG Unconventional Resources Technology Conference*, 2018 https://doi.org/10.15530/URTEC-2018-2879569

[19] Z. Wang, and R. Wang, "Pore pressure prediction using geophysical methods in carbonate reservoirs: Current status, challenges and way ahead," *Journal of Natural Gas Science and Engineering*, vol. 27, no. 2, pp.986-993, 2015. https://doi.org/10.1016/j.jngse.2015.09.032

[20] J. Zhang, "Pore Pressure Prediction from Well Logs: Methods, Modifications, and New Approaches," *Earth Science Review*, vol. 108, no. 1-2, pp. 50-63, 2011. https://doi.org/10.1016/j.earscirev.2011.06.001

[21] R.W. Zimmerman, "Compressibility of sandstones," Developments in Petroleum Science, vol. 29, Elsevier Science Pub. Co., 183 pp, 1991. ISBN 978-0444883254.

[22] B. Aadnoy, and R. Looyeh, "Petroleum rock mechanics: drilling operations and well design," Gulf professional publishing, 2019.

[23] Schlumberger, "Techlog Pore Pressure Prediction and Wellbore Stability Analysis Workflow / Solutions Training," 2015.

[24] M. Thiercelin, and R. A. Plumb, "Core-based prediction of lithologic stress contrasts in east Texas formations," SPE Formation Evaluation," vol. 9, pp. 251-258, 1994. https://doi.org/10.2118/21847-PA

التحقيق في عدم استقرار البئر في جنوب حقل الرميلة النفطي

علي فرج زيدان [١،*]، فرقد علي هادي [١]، مارتن كليمبا [٢]

١ قسم هندسة النفط، كلية الهندسة، جامعة بغداد، بغداد، العراق

٢ قسم هندسة الجيولوجيا، كلية التعدين والجيولوجيا، جامعة اوسترافا التقنية، اوسترافا، التشيك

الخلاصة

تهدف هذه الدراسة إلى معالجة مشكلة عدم استقرار حفرة البئر في جنوب حقل الرميلة النفطي من خلال توفير رؤى قيمة للعوامل المساهمة في عدم استقرار حفرة البئر واقتراح تدابير فعالة للتخفيف من المشكلة في الجزء الجنوبي من حقل الرميلة النفطي. تم تطوير نموذج أرضي ميكانيكي أحادي البعد (MEM ١D) من خلال استخدام سجلات مختلفة من اربعة ابار موزعة عبرجنوب الحقل، بما في ذلك أشعة جاما وحجم البت والفرجار والكثافة والضغط الصوتي وسجلات القص. تم التحقق من صحة النموذج من خلال الاختبارات المعملية، بما في ذلك حلمات Brazilin و Triaxial، بالإضافة إلى اختبارات التكوين المتكررة. لتحليل استقرار حفرة البئر، تم استخدام ثلاثة معايير فشل مختلفة، وهي Mohr–Coulomb وMogi–Coulomb و Modified lade. تم إجراء التحليل باستخدام سجلات الفركجر، وأشارت النتائج إلى أن معيار Mogi–Coulomb كان معيار الفشل الأكثر دقة في التنبؤ بانهيار الصخور. وقد لوحظت مشاكل عدم استقرار حفر الآبار عبر أقسام الصخر الزيتي في جميع أنحاء حقل الرميلة النفطي، وخاصة من خلال تنومة، والخصيب، وأعلى وأسفل الأحمدي ، ونهر عمر وعضو الصخر الزيتي العلوي والعضو الصخري الأوسط في تشكيلات الزبير.اشارت نتائج (MEM ١D) إلى أن تشكيلات (Shaly) أظهرت صخورًا منخفضة الصلابة (معامل يونغ منخفض YME)، وقوة صخرية منخفضة ونسبة بواسون عالية (PR) ، مما يشير إلى وجود تحديات محتملة تتعلق بعدم استقرار حفرة البئر في تنومة، أعلى وأسفل الأحمدي، نهر عمر والزبير. تم إجراء تحليل الحساسية لتحديد أسلم وزن للطين والمسار الأمثل للبئر لعمليات الحفر المستقبلية. ووفقًا للنافذة الطينية المحدثة لهذا الحقل في عام ٢٠٢٣، فقد تم تعزيز الضغط في تكوينات مشرف والزبير بآبار الحقن ، حيث لوحظ أن سلوك الضغط قد تحول من النضوب (٢٠٠٠ رطل لكل بوصة مربعة). بناءً على نتائج هذه الدراسة، يمكن حفر ميل البئر (٠–٢٥ درجة) بوزن طين يتراوح بين ١,٢٤–١,٢٦ جرام ، بينما يمكن حفر ميل البئر (٢٥–٤٠ درجة) بوزن الطين البالغ ١,٢٨–١,٣٠ ج في جميع الاتجاهات (أي جميع السمت). وجد أن نظام الضغط في غالبية التشكيلات كان بمثابة انزلاق إضراب إلى نظام الخطأ العادي. يمكن لنتائج هذه الدراسة أن تفيد صناعة النفط بشكل كبير وتعزز الإنتاجية الإجمالية.

الكلمات الدالة: حقل الرميلة النفطي، عدم استقرارية جدار البئر، طبقة الشيل، نافذة الطين.